공학석사 학위논문

CAV Control Strategy at a Freeway Lane-drop Bottleneck Considering the Gap Settings of AVs

AV의 Gap Settings를 고려한 고속도로 Lane-drop Bottleneck에서의 CAV 제어 전략 개발

2023년 2월

서울대학교 대학원
공과대학 건설환경공학부

정 성 용

CAV Control Strategy at a Freeway Lane-drop Bottleneck Considering the Gap Settings of AVs

지도 교수 이 청 원

이 논문을 공학석사 학위논문으로 제출함

2022년 12월

서울대학교 대학원
공과대학 건설환경공학부

정 성 용

정성용의 공학석사 학위논문을 인준함

2023년 1월

위 원 장 김 동 규 (인)

부위원장 이 청 원 (인)

위 원 고 승 영 (인)

Abstract

Lane-drop bottleneck is a frequently observed bottleneck in a freeway due to lane closures, work zones, and incidents. A potential cause for a capacity drop at a lane-drop bottleneck is the critical conflicts by mandatory lane changing near the lane-dropping point, and the upstream inflow higher than the downstream capacity. Therefore, the throughput is expected to increase by operating CAV control strategy that can reduce disruption and keep the upstream inflow under downstream capacity. CAVs in this study are assumed to provide multiple gap settings, including the shortest and the longest gap settings currently available in commercial AVs. A novel concept that controls the gap setting of CAVs to increase throughput at a lane-drop bottleneck is proposed. The proposed strategy consists of merging control and inflow control. Merging control adjusts the gap setting of CAVs to a proposed gap setting that can reduce disruption caused by merging when applied to CAVs. Inflow control adjusts the gap setting of CAVs to either the shortest or the longest gap setting dynamically to regulate upstream inflow and keep bottleneck occupancy at the target occupancy. Proportional-Integral-Derivative (PID) controller was utilized for inflow control. To validate the proposed strategy, the simulation experiment was conducted with micro-simulation VISSIM. The results indicated that the proposed strategy prevents capacity drop and improves traffic flow efficiency in all demand scenarios under CAV environment. The proposed strategy also improved traffic flow efficiency under all simulated MPR scenarios, and the gain in performance was marginal for MPRs higher than 50%. Furthermore, the proposed strategy reduced CO_2 emissions and the number of conflicts for all MPRs.

Keyword: Gap Setting, CAV, Lane-drop Bottleneck, Proportional-Integral-Derivative Control, VISSIM

Student Number: 2019-27105

Table of Contents

List of Tables

List of Figures

Chapter 1. Introduction

Lane-drop bottleneck is a frequently observed bottleneck in a freeway due to lane closures, work zones, and incidents (Jin and Jin, 2015; Guo et al., 2020). At a lane-drop bottleneck, the capacity of the downstream is lower than that of the upstream as the number of lanes decreases. Therefore, the upstream inflow of the bottleneck is likely to exceed the downstream capacity during peak hours. This situation may lead to a capacity drop; which refers to the state when the maximum throughput is lowered than the downstream capacity (Jin and Jin, 2015; Yuan et al., 2015; Zhang and Ioannou, 2016). Another potential cause of a capacity drop is the critical conflicts by mandatory lane changing near the lane-dropping point (Zhou et al., 2017; Hu and Sun, 2019; Guo et al., 2020).

The capacity drop still occurs even in the existence of Automated Vehicles (AVs). Commercial AVs provide multiple gap settings that can be adjusted by drivers while driving. Tesla, for example, provides seven gap settings and Hyundai provides four gap settings. All car makers reviewed in this study including BMW, Mercedes-Benz, AUDI, and Toyota also provide multiple gap settings. Shi and Li (2021) found that compared to Human-Driven Vehicles (HDVs), AVs with the shortest gap setting have a shorter average time gap, and longer average time gap with the longest gap setting. Therefore, the capacity is expected to be significantly increased when all AVs drive with the shortest gap setting. However, the capacity drop may still occur at the lane-drop bottleneck due to large upstream inflow and lane changing, as mentioned above, meaning that the throughput would still be lower than the downstream capacity. Consequently, even with the technology of AVs that allows driving with a small gap (Ren et al., 2020), there still is room for improvement in terms of throughput at the lane-drop bottleneck with traffic management and control.

To improve the operational efficiency of traffic flow, the cooperation of individual vehicles based on the global condition is required (Ren et al., 2020). Connected and Automated Vehicles (CAVs) not only allow to operate in isolation with internal sensors but can also make cooperative decisions via communication with the surrounding vehicles and the infrastructures nearby (Wang et al., 2018). Especially, the benefits of these technologies are even more prominent in freeway bottlenecks where frequent lane changing, merging, and yielding maneuvers occur (Hu and Sun, 2019).

Various studies proposed CAV control strategies that facilitate smooth merging in freeway bottlenecks. Some studies proposed optimization-based methods that optimize the accelerations of CAVs to improve the efficiency at the bottlenecks (Chen et al. 2020; Karimi et al., 2020; Min et al., 2020). Others proposed strategy-based methods that design rules that can be applied to CAVs for smooth merging (Lu and Hedrick., 2003; Zhou et al., 2016; Bang and Ahn, 2018). However, controlling individual vehicles can only benefit from local and microscopic levels, since it does not consider macroscopic control in traffic flow level (Zhu et al, 2022).

Another mainstream of traffic management at the freeway bottleneck is regulating the upstream inflow of the bottleneck considering the macroscopic traffic flow characteristics. The upstream inflow can be indirectly controlled by adjusting the speed limit of vehicles (Variable Speed Limit, VSL), or by controlling the ramp metering rates (Ramp Metering, RM). However, these algorithms only control macroscopic traffic flow characteristics in an aggregate and inaccurate way (Hu and Sun, 2019; Zhu et al., 2022). Therefore, the operation at the bottleneck is expected to be further improved when CAVs are controlled appropriately with the consideration of both microscopic merging maneuvers and macroscopic traffic flow characteristics.

This study aims to develop a novel CAV gap setting control strategy that can relieve or even prevent congestion at the lane-drop bottleneck. The CAVs in this study are assumed to provide multiple gap settings, including the shortest and the longest gap settings

currently available in commercial AVs. Also, it is assumed that the gap setting of CAVs can be controlled by the traffic management center by V2I communications. The proposed strategy consists of merging control and inflow control. Merging control applies a new gap setting to CAVs to reduce oscillation caused by merging. Inflow control changes the gap setting of CAVs to either the shortest or the longest gap setting dynamically to regulate the upstream inflow and keep the bottleneck occupancy at the target occupancy. The main contributions can be summarized as follows:

- Car-following models for both the shortest and the longest gap settings of commercial AVs were calibrated using real-world data
- A novel concept that controls the gap setting of CAVs is proposed
- The proposed strategy considers both microscopic merging maneuvers and macroscopic traffic flow characteristics
- A platform based on Python, VISSIM COM, and C++ is developed to implement the proposed strategy
- The results showed that the proposed strategy can prevent capacity drop and reduce travel time in all simulated traffic demand scenarios under CAV environment
- The proposed strategy improved traffic efficiency for all MPRs under mixed-traffic environment of CAVs and HDVs
- The proposed strategy also reduced CO_2 emissions and the number of conflicts for all MPRs

Chapter 2. Literature Review

2.1. Microscopic Control Algorithms

Many studies that control CAVs located near a bottleneck to facilitate smooth merging have been presented. These works can be roughly classified into two types: strategy-based and optimization-based methods (Hu and Sun, 2019).

In strategy-based methods, many rules that can be applied in various circumstances are designed with a common goal to obtain a smooth merging maneuver. First, some studies control the car-following model parameters of CAVs near the merging area. These studies assume that the car-following model parameters of CAVs can be set differently depending on the situation. Zhou et al. (2016) proposed CIDM-based AV that the car-following parameters are set depending on the merging condition. They showed that the proposed AV can relieve freeway oscillations. Bang and Ahn (2018) proposed a method that can resolve a disturbance created by a merging vehicle by controlling two parameters, the spring constant and the damping coefficient, of the SMD-based control model under a full CAV environment. Ren et al. (2020) showed an appropriate gap can be formed for the merging vehicle by controlling the VISSIM car-following parameters. However, the parameters controlled in the studies mentioned above may significantly differ from the commercial AVs and may show unrealistic or uncomfortable behavior with the set parameters.

Additionally, several studies tried to solve the on-ramp merging problem with a virtual vehicle mapping technique. These works converted on-ramp merging maneuvers to car-following tasks (Liang et al., 2022). Lu and Hedrick (2003) proposed a virtual vehicle following concept that can form a platoon effectively in two topologies (i.e. either with or without an acceleration lane). Hu et al. (2021) determined a merging sequence based on the estimated merging point arrival time and proved that merging efficiency can be improved by

each vehicle following the preceding vehicle defined in the merging sequence. Chen et al. (2021) converted the on-ramp merging problem into a car-following problem at a virtual axle, that is based on a virtual car-following sequencing through a virtual rotation technique. Through numerical simulation, the authors showed that the proposed control can reduce voids and guarantee to dampen traffic oscillation. However, since the majority of strategy-based methods are decentralized, optimal control for the merging system cannot be achieved (Zhou et al., 2018; Hu and Sun, 2019; Zhu et al. 2022).

On the other hand, the majority of the works deploying optimization-based methods assume that the acceleration of CAVs can be controlled by the traffic management center. These studies calculate the appropriate acceleration for each CAV to form a merging gap to maximize or minimize the objective function. Cao et al. (2015) proposed a predictive control-based optimization model that can successfully generate a cooperative merging path in a typical traffic situation. Karimi et al. (2020) calculated the appropriate acceleration of CAVs in mixed traffic flow, depending on the combinations of CAVs and HDVs in a merging triplet of the subject vehicle, lead vehicle, and lag vehicle. The prediction has been made to predict the behavior of HDVs. Other studies (Rios-Torres et al., 2016; Min et al., 2020; Chen et al. 2020) also presented strategies for CAV acceleration rate determination under CAV 100% environment and evaluated the performance by numerical simulation. However, in an environment where the traffic management center controls the acceleration rate of all CAVs, the safety of the vehicles can be critically jeopardized when communication is delayed or failed. Also, the assumption that the acceleration of the CAVs can be controlled by the traffic management center completely ignores the current decentralized driving behavior of AVs that relies on internal sensor information. Therefore, full acceleration rate control by the traffic management center is expected to be possible in the very distant future. Furthermore, controlling individual vehicles can only benefit from local and microscopic levels, since macroscopic control in traffic flow level is not considered (Zhu et al., 2022).

2.2. Macroscopic Control Algorithms

Other strategies implemented in a freeway bottleneck control the upstream inflow of the bottleneck from a macroscopic viewpoint to improve flow efficiency. The upstream inflow can be indirectly controlled by controlling the speed limit of the vehicles (VSL), or by controlling the ramp metering rate at the ramp located upstream of the bottleneck (RM). The control of upstream inflow depending on the traffic state has been proven to improve traffic flow efficiency.

Khondaker and Kattan (2015) used microsimulation VISSIM to verify that travel time can be reduced by controlling the speed limit of Connected Vehicles (CVs). Müller et al. (2015) evaluated both point VSL and space VSL, and concluded that both strategies can improve traffic conditions where space VSL performs better than point VSL. Jin and Jin (2015) controlled the upstream speed limit using a PI controller and numerically showed that travel time can be decreased by up to 86%. Wu et al. (2020) developed a deep-reinforcement learning-based lane-specific speed limit selection method and proved its effectiveness using microsimulation SUMO. The aforementioned studies have verified the usefulness of controlling the speed of the vehicles located upstream of the bottleneck in relieving congestion.

Another strategy that controls upstream inflow is a well-known RM system. Papageorgiou et al. (1991) presented ALINEA and found that occupancy could be maintained near critical occupancy with the metering rate calculated by the P controller. Also, Wang et al. (2014) showed PI-ALINEA can effectively improve the traffic state with an active bottleneck downstream of the merging area.

However, these algorithms only control macroscopic traffic flow characteristics in an aggregate and inaccurate way (Hu and Sun, 2019; Zhu et al., 2022). Therefore, the operation at the bottleneck is expected to be further improved when macroscopic inflow control is combined with microscopic merging control in CAV environment.

2.3. Impact of AV on Traffic Flow

Adaptive Cruise Control (ACC) systems, that control the longitudinal behavior of AVs, are now largely available in commercial vehicles. Changing the car-following dynamics can have a large impact and therefore, there have been efforts to analyze the impact of AV on traffic flow.

Many studies analyzed the impact of AVs based on the assumed driving behavior. Davis (2004) assumed string stable AV and showed that on-ramp jam is prevented with an AV penetration rate higher than 20%. Kesting et al. (2010) found that AVs modeled by Intelligent Driver Model (IDM), which adjusts the parameters depending on the situation, can increase capacity. Talebpour and Mahmassani (2016) analyzed stability and throughput in a mixed flow of HDV, CV, and AV and claimed that both CV and AV improve stability and throughput. Calvert et al. (2017) assumed AV modeled by IDM and found AV can have a negative effect on flow with low MPR. Zhu and Zhang (2018) found that when density is lower than the critical value, both throughput and stability improve with the increase of AV. However, AV may negatively affect throughput when density is higher than the critical value. Although the aforenoted works quantitively analyzed the effects of AV in a mixed environment, the results are highly dependent on the assumed behavior of AVs so the results can change significantly when the model is calibrated with commercial AV data.

To fill this gap, recent studies evaluated the impact of AVs by utilizing the trajectory data of commercial AV datasets. Gunter et al. (2020) analyzed the string stability using the trajectory data of seven commercial AVs and concluded that they are all string unstable for both the shortest and longest gap settings. Makridis et al. (2020) evaluated the trajectory data of the platooning experiment with five commercial AVs. 23 experiments all showed that the vehicles are string unstable. Shang and Stern (2021) compared string stability and capacity calibrated by theoretical AV and commercial AV. They found that theoretical AV improves both string stability and capacity, whereas commercial AVs are string unstable and can reduce

bottleneck capacity with a high penetration rate. The findings of Shi and Li (2021), evaluated with the commercial AV dataset, showed that the shortest gap setting of AVs can increase capacity significantly compared to that of HDV, and the longest gap setting relatively reduces the capacity.

In summary, recent studies analyzing commercial AVs showed a discrepancy between theoretically assumed AVs and commercial AVs. Also, although most studies analyzing the impact of AV assumed homogeneous longitudinal behavior of AVs, commercial AVs offer multiple gap settings meaning that the longitudinal behavior of AVs can differ significantly depending on the gap setting.

Therefore, this study aims to develop a realistic CAV control strategy by considering the longitudinal dynamics of commercial AVs depending on the gap settings. CAVs are assumed to provide gap settings including the shortest and the longest gap settings currently provided in commercial AVs. A novel strategy that controls the gap setting of CAVs is proposed in this study so as to reduce disruption caused by merging and to regulate the upstream inflow appropriately. A detailed description of the proposed strategy is introduced in the following chapter.

Chapter 3. Methodology

3.1. Vehicle Modeling

3.1.1. Car-Following Models

This study focused on the fact that commercial AVs provide multiple gap settings that perform significantly different longitudinal behavior. To develop a realistic CAV control strategy, this study calibrated a car-following model that can represent the longitudinal maneuver of AVs with different gap settings, and assumed that CAVs also provide multiple gap settings including those equipped in current commercial AVs. For the car-following model selection, the models that were frequently applied for modeling (C)AVs were compared.

In the previous studies, various car-following models were adopted for modeling the longitudinal car-following behaviors of vehicles, including HDV, AV, CV, and CAV. The car-following models used in the previous studies for various types of vehicles are summarized in Table 3.1.

Table 3.1 Car-following models used in previous studies

Authors (Year)	Car-Following Models			
	HDV	CV	AV	CAV
Kesting et al. (2010)	IDM	-	IDM	-
Talebpour and Mahmassani (2016)	Talebpour (2011)	IDM	Van Arem (2006)	-
Monteil et al. (2018)	IDM	-	-	IDM
Zheng et al. (2020)	OVM	-	OVM	-
Gunter et al. (2020)	-	-	FVDM	-
Yao et al. (2021)	IDM	-	-	IDM

Three car-following models (OVM, FVDM, and IDM) frequently applied for (C)AV modeling were selected for commercial AV modeling in this study.

Bando et al. (1995) developed the Optimal Velocity Model (OVM). Mathematically, the model can be expressed as

$$\ddot{x_n} = a\left[v_{opt}(x_{n-1} - x_n) - \dot{x_n}\right] \quad (3.1)$$

where,

$\ddot{x_n}$ = acceleration applied by driver n,
a = sensitivity constant,
$v_{opt}(s)$ = desired velocity function,
$\dot{x_n}$ = the speed of vehicle number n,
x_n = the coordinate of the vehicle number n,
x_{n-1} = the coordinate of the preceding vehicle.

Various desired velocity functions, $v_{opt}(s)$, were used in previous studies, with the common fact that the desired velocity depends on the relative position of the vehicle (Aghabayk et al., 2015). In this study, the desired velocity function presented by Trieber and Kesting (2013) shown in Equation 3.2 was chosen.

$$v_{opt}(s) = \max\left[0, min\left(v_0, \frac{x_{n-1} - x_n - s_0}{T}\right)\right] \quad (3.2)$$

Where,

v_0 = desired speed,
s_0 = minimum gap,
T = time gap.

The OVM, however, encounters the problems of generating unrealistic acceleration and deceleration values (Jiang et al., 2001).

To present a more realistic model, Jiang et al. (2001) introduced the Full Velocity Difference Model (FVDM) which takes both positive and negative velocity differences into account. Mathematically, the model can be expressed as

$$\ddot{x_n} = \kappa\left[v_{opt}(x_{n-1} - x_n) - \dot{x_n}\right] + \lambda(\dot{x_{n-1}} - \dot{x_n}) \quad (3.3)$$

Where,

$\ddot{x_n}$ = acceleration applied by driver n,
κ = sensitivity constant,
λ = sensitivity constant,
$v_{opt}(s)$ = desired velocity of vehicle number n,

$\dot{x_n}$ = the velocity of vehicle number n,
$\dot{x_{n-1}}$ = the velocity of the preceding vehicle,
x_n = the coordinate of the vehicle number n,
x_{n-1} = the coordinate of the preceding vehicle.

For modeling the longitudinal behavior of commercial AV, the desired velocity function in Equation 3.2 is also applied for the FVDM, and the calibrated parameters are presented in the following section.

This model has a limitation in describing all traffic situations. Specifically, since the term $\lambda(\dot{x_{n-1}} - \dot{x_n})$ is not dependent on the gap, a slow preceding vehicle far away leads to significant unrealistic decelerating behavior of the following vehicle (Trieber and Kesting, 2013).

The last car-following model considered in this study is the Intelligent Driver Model (IDM). The model can be expressed as

$$\ddot{x_n} = \alpha \left(1 - \left(\frac{\dot{x_n}}{v_0} \right)^{\delta} - \left(\frac{s_0 + T\dot{x_n} - \frac{\dot{x_n}(\dot{x_{n-1}} - \dot{x_n})}{2\sqrt{\alpha\beta}}}{s_n} \right)^2 \right) \quad (3.4)$$

Where,

$\ddot{x_n}$ = acceleration applied by driver n,
v_0 = desired speed,
s_0 = minimum gap,
s_n = distance gap.
T = time gap.
α = maximum acceleration,
β = comfortable deceleration,
δ = acceleration exponent,
$\dot{x_n}$ = the velocity of vehicle number n,
$\dot{x_{n-1}}$ = the velocity of the preceding vehicle.

IDM is an accident-free model that produces realistic acceleration profiles, and each model parameters describe only one aspect of the driving behavior which is favorable for the model calibration (Trieber and Kesting, 2013). Thus, this model has been

implemented in micro-simulation in several studies (Guériau et al., 2016; Talebpour and Mahmassani, 2016; Zhu et al., 2018; Rahman et al., 2019).

3.1.2. Parameter Calibration

Recent studies showed that the car-following model parameters can be calibrated with high-resolution trajectory data of the vehicles. Punzo et al. (2021) reviewed objective functions for the previous studies and found they varied widely. An objective function for the car-following model calibration can be defined with the Goodness-of-Fit function (GoF) and Measure-of-Performance (MoP). The authors compared possible combinations of 7 GoFs and 4 MoPs and the results were consistent that regardless of the GoF, the model, and the dataset, spacing is preferable as MoP. Also, focusing on spacing, GoFs which are not based on percentage errors are always preferable to percentage-based GoFs. Therefore, this study applied spacing as GoF, and Root Mean Squared Error (RMSE) as MoP for parameter calibration as in Equation 3.5, with a gradient-based optimization method used for calibration.

$$\text{minimize} \sqrt{\frac{1}{T}\sum_{t=1}^{T}[s^{est}(t) - s^{obs}(t)]^2} \tag{3.5}$$

Where,

T = number of time steps,
t = a time step,
$s^{est}(t)$ = estimated spacing at time step t,
$s^{obs}(t)$ = observed spacing at time step t.

3.2. Gap Setting Control Strategy

The objective of the proposed strategy is to improve throughput at a lane-drop bottleneck by controlling the gap setting of CAVs located near the lane-drop bottleneck. The proposed strategy consists of merging control and inflow control and is operated within section 1 to section 3 (**Figure 3.1**).

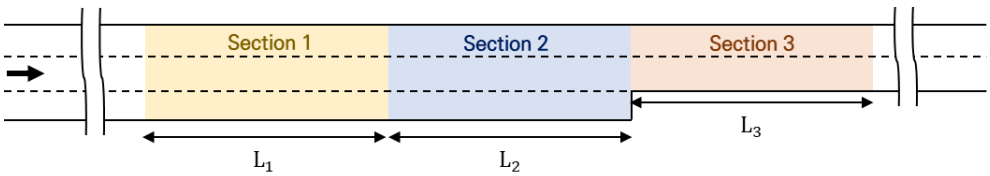

Figure 3.1. Overview of the control region

Merging control instructs CAVs, located in the center lane and the merge lane in section 2 of **Figure 3.1**, to change gap setting to the proposed gap setting. It is a microscopic control strategy that relieves disruption caused by mandatory merging in section 2. Inflow control is a macroscopic control strategy that controls the gap setting of CAVs entering section 1 to regulate the upstream inflow and keep bottleneck occupancy at the target occupancy. Outside the control region, CAVs remain uncontrolled with a gap setting set by the driver's preference.

3.2.1. Merging Control

Merging control changes gap setting of CAVs, located in the center lane and the merge lane in section 2, to a proposed gap setting to reduce disruption caused by merging. As shown in **Figure 3.2**, when a proposed gap setting is applied, the CAV in the center lane in section 2 follows both the preceding vehicle in the center lane and the preceding vehicle in the merge lane. The same logic is applied to CAV in the merge lane, following both the preceding vehicle in the merge lane and the center lane.

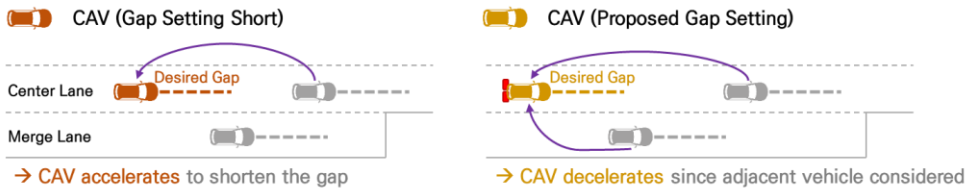

Figure 3.2. Conceptual diagram of merging control

A car-following model for the proposed gap setting that is designed to be applied for CAVs on the center lane and the merge lane in section 2 is described in Equation 3.6 and Equation 3.7.

$$\ddot{x_n} = min\left(a_{Same\ Lane},\ max\left(-2,\ a_{Adjacent\ Lane}\right)\right) \tag{3.6}$$

$$a_j = \alpha\left(1 - \left(\frac{v_n}{v_0}\right)^{\delta} - \left(\frac{S_0 + Tv_n + \frac{v_n\Delta v}{2\sqrt{\alpha\beta}}}{S_n}\right)^2\right), \quad j = \begin{cases} Same\ Lane \\ Adjacent\ Lane \end{cases} \tag{3.7}$$

Where,

v_0 = desired speed,
s_0 = minimum gap,
s_n = distance gap between preceding vehicle and subject vehicle,
Δv = relative speed between preceding vehicle and subject vehicle,
T = time gap,
α = maximum acceleration,
β = comfortable deceleration,
δ = acceleration exponent.

In a case where there only exists a preceding vehicle in the same lane within a detection range of CAV, the original car-following model is applied (Equation 3.8).

$$\ddot{x_n} = \alpha\left(1 - \left(\frac{v_n}{v_0}\right)^{\delta} - \left(\frac{S_0 + Tv_n + \frac{v_n\Delta v}{2\sqrt{\alpha\beta}}}{S_n}\right)^2\right) \tag{3.8}$$

Likewise, in a case where there only exists a preceding vehicle in an adjacent lane within a detection range of CAV, CAV would follow

a preceding vehicle in an adjacent lane with original car-following logic with a minimum deceleration of $-2\,\mathrm{m}/s^2$ for a comfortable deceleration (Equation 3.9).

$$\ddot{x_n} = max\left(-2,\ \alpha\left(1-\left(\frac{v_n}{v_0}\right)^{\delta}-\left(\frac{S_0+\ Tv_n+\ \frac{v_n\Delta v}{2\sqrt{\alpha\beta}}}{S_n}\right)^2\right)\right) \tag{3.9}$$

Lastly, if no preceding vehicles exist for both current and adjacent lanes, CAV would accelerate until the free flow speed is reached (Equation 3.10).

$$\ddot{x_n} = \alpha\left(1-\left(\frac{v_n}{v_0}\right)^{\delta}\right) \tag{3.10}$$

By applying the proposed gap setting to CAVs on both the center lane and the merge lane, a CAV would decelerate considering both preceding vehicles when present, if one of the current time gaps with the preceding vehicles is smaller than the desired time gap. Thereby, enough gap for merging will be formed, so the oscillation caused by a merging vehicle is expected to decrease. For all four situations mentioned above, the corresponding parameters are set with the calibrated shortest gap setting parameters of commercial AVs to maximize throughput. Note that the proposed gap setting can also be applied in a mixed traffic flow of CAVs and HDVs. Regardless of the vehicle type of preceding vehicles, a CAV would follow two preceding vehicles if preceding vehicles in both lanes exist.

The gap settings of CAVs in the median lane of section 2 and in section 3 are switched to the shortest gap setting, maximizing the capacity of the controlled regions near the lane-dropping point. If the length of section 2 (L_2) is too short, the desired gap for CAVs considering the vehicles in the adjacent lane may not be formed before merging. Finding a proper length for section 2, however, is beyond the scope of this study. Despite the improvement in merging behaviors through the operation of merging control, the control does not guarantee the optimum operation in any sense since it does not

consider macroscopic traffic flow characteristics.

3.2.2. Inflow Control

From a macroscopic traffic flow perspective, bottleneck flow efficiency can be improved by keeping the bottleneck occupancy or density at a target value, such as critical occupancy. Inflow control tries to keep the bottleneck occupancy at the target occupancy by adjusting the gap setting of CAVs entering section 1 to either the shortest or the longest gap setting. To successfully control the inflow, this study applied a Proportional–Integral–Derivative (PID) controller, which is widely used in industrial control. As shown in Figure 3.3, a PID controller determines the input value based on the error between the output and the target value.

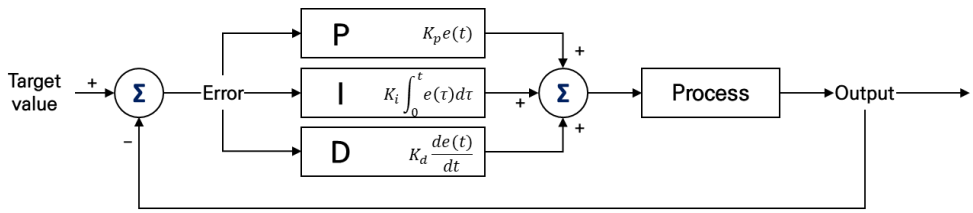

Figure 3.3. Conceptual diagram of PID control

This study applied a discrete time PID controller to determine the desired short gap setting ratio, $p_{S,des}(k)$ (Figure 3.4). The gap setting of a CAV is controlled to either the shortest gap setting (namely, short gap setting) or the longest gap setting (namely, long gap setting) to match the current short gap setting ratio in section 1 to the desired value, $p_{S,des}(k)$. The equation for the discrete time PID controller is as follows (Equation 3.11–3.15).

$$p_{S,\,des}(k) = p_{S,\,des}(k-1) + K_0 e(k) + K_1 e(k-1) + K_2 e(k-2) \quad (3.11)$$

$$e(k) = occ_{target} - occ(k) \quad (3.12)$$

$$K_0 = K_P + K_I T + K_D T^{-1} \quad (3.13)$$

$$K_1 = -K_P - 2K_D T^{-1} \quad (3.14)$$

$$K_2 = K_D T^{-1} \quad (3.15)$$

Where,

$p_{S,des}(k)$ = desired short gap setting ratio at time kT,
T = discrete time step (e.g., 1 second),
k = sample time index (0, 1, 2, ···),
$e(k)$ = error at time kT,
$occ(k)$ = occupancy at time kT,
occ_{target} = target occupancy,
K_P, K_I, K_D = PID parameters.

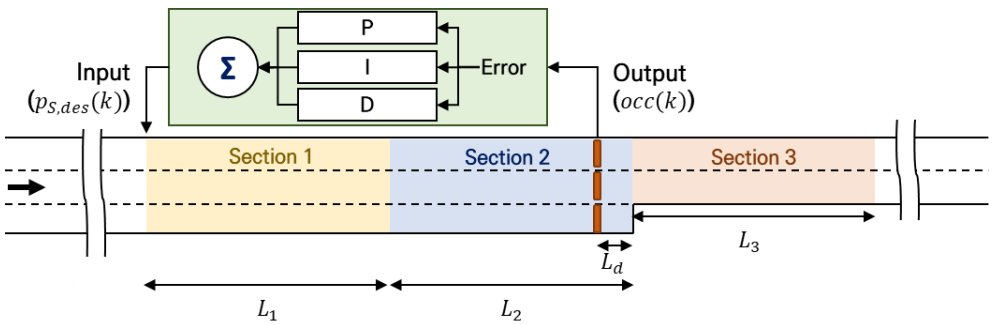

Figure 3.4. Conceptual diagram of inflow control

If the current occupancy is smaller than the target occupancy ($e(k) > 0$), the controller would increase the desired short gap setting ratio to increase upstream inflow. In the opposite situation, the desired short gap setting ratio would be decreased to reduce upstream inflow. The loop detector is located upstream of the lane-dropping point to sensitively detect the formation of the queue and the capacity drop. If L_d, the distance from the lane-dropping point, is too long, the controller would not be able to prevent the formation of a queue. Finding the optimal location for the loop detector is not considered in this study.

The gap settings of CAVs entering section 1 are adjusted via V2I communication with the traffic management center. Note that the gap setting for each CAV is adjusted at most once in section 1. Also, lane changing in section 1 is prohibited to allow CAVs to accelerate without disturbance when the queue forms upstream of section 1. If the length of section 1 (L_1) is too short, the space for acceleration may be insufficient. If the length is too long, a disturbance may occur

frequently between the starting point of section 1 and the point where the loop detector is located. The optimal value of L_1 is outside the scope of this study.

3.2.3. Combination of Merging Control and Inflow Control

The proposed strategy that considers both microscopic and macroscopic control themes at a lane-drop bottleneck is proposed. First, merging control is always operated to reduce disruption caused by mandatory lane changing. However, when upstream inflow exceeds downstream capacity, the capacity drop that lowers the throughput than the capacity can still occur, as shown in Figure 3.5.

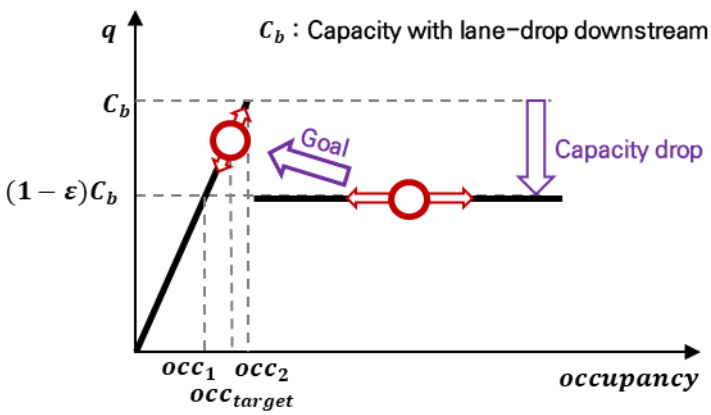

Figure 3.5. Theoretical MFD at the upstream section of the lane-drop bottleneck

Inflow control is combined with merging control to regulate bottleneck inflow when the capacity drop cannot be prevented by operating merging control only. Inflow control is operated when $occ(k) > occ_1$, and the target occupancy (occ_{target}) is set between occ_1 and occ_2 as in Figure 3.5. The objective of inflow control is to keep occupancy at the target occupancy to keep throughput over $(1-\varepsilon)C_b$ without turning into a congested state. Note that adjusting PID parameters and the target occupancy can further improve the operational benefits of the proposed strategy. The optimal tuning for those parameters is out of the scope of this study. Figure 3.6 shows

the flowchart of the proposed strategy.

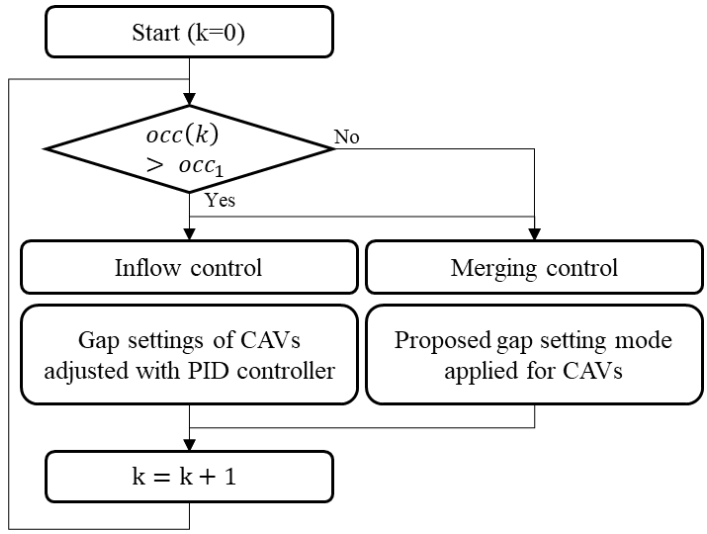

Figure 3.6. Flow chart of the proposed strategy

Chapter 4. Simulation Analysis

4.1. Simulation Design

4.1.1. Vehicle Modeling

This study evaluated the performance of the proposed strategy via microsimulation VISSIM, with a platform based on Python, VISSIM COM, and C++ External Driver Model. Both macroscopic and microscopic results can vary significantly depending on the behaviors of CAVs and HDVs modeled in the simulation. Therefore, reasonable modeling of CAVs is quite important.

As mentioned previously, this study assumed that the gap settings of CAVs can be controlled by the traffic management center in the control region to improve the efficiency of the traffic flow. It was also assumed that CAVs provide gap settings, including short and long gap setting. Since the longitudinal behavior of CAVs depending on the gap setting differs significantly, the car-following model for each setting was calibrated separately from high-resolution trajectory data of commercial AVs.

To calibrate the commercial AVs' longitudinal driving behavior, the AstaZero test track data included in the Open ACC database was utilized in this study. The Open ACC database consists of car-following experiments that involve vehicles with ACC systems. Although there are 7 datasets available in the Open ACC database, the car-following dataset that was tested on the 5.7km long AstaZero test track in Sweden was chosen for two reasons. Firstly, unlike the conventional dataset, this dataset includes both starting from a standstill and stopping, allowing more precise calibration for the car-following models. Secondly, unlike the other datasets that only include the shortest gap setting, each high-end commercial AV was tested with both the shortest and longest gap setting.

The car-following experiment taken in the AstaZero test track was conducted in the second quarter of 2019. Five high-end vehicles

were involved in the experiment, from four different makes and all different models (Table 4.1). In all tests, the leader vehicle, AUDI A8, was followed by the four vehicles in various order with the ACC enabled with either the short or long gap setting available.

Table 4.1 Vehicle specification

Vehicle Model	Max Power (kW)	Drive-Fuel	Model Year
AUDI A8 (Leader)	250	Diesel	2018
TESLA Model 3	150	Electricity	2019
BMW X5	195	Diesel	2018
MERCEDES A Class	165	Gasoline	2019
AUDI A6	150	Diesel	2018

The trajectory data of the vehicles were collected with the system called RT-Range S multiple target ADAS measurements solution by Oxford Technical Solutions Company. This system provides a frequency higher than 100Hz, so the collected data was processed with down sampling to achieve 10 Hz. The dataset includes the speed, latitude, longitude, and distance gap as shown in Table 4.2.

Table 4.2 AstaZero data columns description

Columns	Unit	Description
Time	s	Common time frame for all vehicles
Speed	m/s	Raw Speed
Lat	Rad	Latitude
Lon	Rad	Longitude
Alt	m	Altitude
E	m	East (x) coordinate in the local ENU plane
N	m	North (y) coordinate in the local ENU plane
U	m	Up (z) coordinate in the local ENU plane
IVS	m	Inter Vehicle Spacing computed from GNSS data after bumper to bumper correction

As mentioned in the previous chapter, spacing was selected as GoF, and RMSE was selected as MoP for the parameter calibration of three car-following models: OVM, FVDM, and IDM. Table 4.3 summarizes the calibration errors for three calibrated car-following models. Root mean squared error for the estimated and observed acceleration, RMSE(a), is shown in the table as a measure for the calibration error. It should be noted that the two parameters that could be extracted straight from the data were fixed before the calibration. Specifically, the minimum gap (s_0) was set by the shortest distance measured in the test data for each vehicle with each gap setting since the dataset includes the stopping of a platoon. Also, the maximum acceleration (α) for IDM was calculated by the 99th percentile value of the observed accelerations. 99th percentile was selected to exclude the unreasonably high maximum acceleration value.

Table 4.3 Calibration errors for car-following models

Vehicle Model (Gap Setting)	Calibration Errors (RMSE(a) [m/s^2])		
	OVM	FVDM	IDM
AUDI A6 (Short)	0.51	0.59	0.46
AUDI A6 (Long)	0.38	0.17	0.19
BMW X5 (Short)	0.40	0.52	0.48
BMW X5 (Long)	0.31	0.25	0.22
MERCEDES A Class (Short)	0.36	0.43	0.51
MERCEDES A Class (Long)	0.24	0.28	0.22
TESLA Model 3 (Short)	0.54	0.46	0.46
TESLA Model 3 (Long)	0.35	0.22	0.31
Average	0.39	0.37	0.36

As mentioned previously, the short gap setting represents the shortest gap setting provided by each vehicle, and the long gap setting represents the longest gap setting provided. The average calibration error for three vehicles shows that IDM has the smallest error. In the following sections, IDM was implemented for modeling

CAVs since it is the only model with the accident-free property among the three models with the smallest calibration error.

To check whether the calibration result is reasonable, string stability analysis is conducted and compared with the results from the previous research. Recently, many studies assessed the impact of AVs concerning string stability, which can be characterized by local stability and string stability. Local stability refers to the stability of a single vehicle's movement over time under the influence of a small perturbation originating from the leading vehicle's movement (Sun et al., 2018). The vehicle is locally stable if the magnitude of the perturbation is smaller in the following vehicle compared to the leading vehicle. In the meantime, string stability, also known as asymptotic stability, focuses on the stability of a platoon of vehicles over space (Sun et al., 2018). When a platoon of vehicles is string unstable, the amplitude of the perturbation, initiated by the leader vehicle, becomes larger as it propagates upstream in the platoon.

Sun et al. (2018) summarized the methods of determining the string stability that can be applied to IDM. The methods include the direct transfer function-based, the Laplace transform-based, and the characteristic equation-based methods. All three methods end up with the same string stability criterion as in Equation 4.1.

$$\frac{1}{2} - \frac{f_{\Delta v}}{f_v} - \frac{f_s}{f_v^2} \geq 0 \tag{4.1}$$

Where,

$$f_s = \left.\frac{\partial a}{\partial s}\right|_e, f_v = \left.\frac{\partial a}{\partial v}\right|_e, f_{\Delta v} = \left.\frac{\partial a}{\partial \Delta v}\right|_e \tag{4.2}$$

are the first-order Taylor expansion coefficients.

The formulation of IDM is shown in Equation 3.4. The Taylor expansion coefficients shown in Equation 4.2 for IDM are formulated as in Equation 4.3-4.5.

$$f_s = \frac{2\alpha}{s_e}\left(\frac{s_0 + Tv_e}{s_e}\right)^2 \tag{4.3}$$

$$f_v = -\alpha\left[\frac{4}{v_0}\left(\frac{v_e}{v_0}\right)^3 + \frac{2T(s_0 + Tv_e)}{{s_e}^2}\right] \tag{4.4}$$

$$f_{\Delta v} = \sqrt{\frac{\alpha}{\beta}} \frac{v_e}{s_e} \frac{s_0 + T v_e}{s_e} \tag{4.5}$$

The calibrated parameters of IDM and the results of string stability analysis are presented in Table 4.4. It shows that all vehicles are string unstable for both short and long gap settings. Also, all vehicles showed improved stability with long gap setting.

Table 4.4 Calibrated parameters for IDM

Vehicle Model (Gap Setting)	v_0 (s)	T (s)	α	β	S_0 (m)	δ	Stable*
AUDI A6 (Short)	50.08	0.96	1.39	5.00	2.27	15.73	−2.88 (X)
AUDI A6 (Long)	37.87	3.34	1.18	3.00	4.62	11.52	−0.34 (X)
BMW X5 (Short)	46.44	1.00	1.31	5.00	1.27	15.41	−2.58 (X)
BMW X5 (Long)	38.29	2.33	1.14	5.00	3.27	12.36	−1.12 (X)
MERCEDES A Class (Short)	56.95	0.90	1.35	5.00	1.75	9.05	−3.02 (X)
MERCEDES A Class (Long)	37.38	2.07	1.00	5.00	3.74	9.92	−1.78 (X)
TESLA Model 3 (Short)	47.19	0.97	1.22	5.00	1.25	13.23	−2.99 (X)
TESLA Model 3 (Long)	38.22	1.98	1.09	3.00	6.23	12.97	−1.50 (X)

* The value stands for the left−hand side of Equation 4.1

It is worth noting that the results of string stability correspond to the previous studies. This supports that the result of the calibration, conducted in this study, is reasonable. Milanés and Shladover (2014) tested with Infinity M56s test vehicle and found that string stability cannot be achieved for a platoon of vehicles using ACC systems. Makridis et al. (2020) analyzed the field test data of five vehicles equipped with ACC that were conducted in AstaZero in Sweden. The study found that the results highlight the instability of the car platoon. Gunter et al. (2020) assessed the string stability of seven commercial ACC−equipped vehicles. All seven vehicles were tested with both the longest and the shortest gap settings, and they modeled the vehicles with FVDM. The results show that all seven vehicles are string unstable under both gap settings. These results

imply that the longitudinal behavior of AV needs improvement regarding string stability. Otherwise, the impact of the string unstable platoon on traffic flow needs to be closely examined, as the number and the length of the AV platoons are expected to increase in the future. More discussions on the string stability of the currently available commercial AVs are out of the scope of this study.

In this study, CAVs with short and long gap settings were modeled by IDM. The average values for each of the calibrated parameters of four vehicles were applied as representative parameters for short and long gap settings, respectively. Vehicles with short and long gap settings were implemented in VISSIM by C++ based External Driver Model. For the modeling of HDVs, VISSIM default parameters (Wiedemann 97, Freeway) were applied. Furthermore, the lateral movements of CAVs and HDVs were handled by VISSIM, assuming the same lateral movements of CAVs as HDVs, due to limitations of obtaining real-world AV data including lateral movements.

4.1.2. Network

This study selected a 6km-long 3 to 2-lane hypothetical lane-drop bottleneck to evaluate the proposed strategy (Figure 4.1). The speed limit is set as 120kph, and the proposed strategy is operated within a 1.5km section. The detector for the inflow control is located 100m upstream from the lane-dropping point.

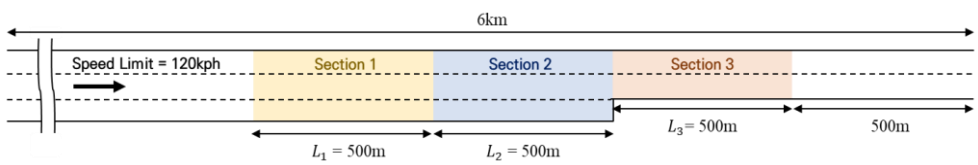

Figure 4.1. Layout of the hypothetical network

As mentioned in the previous chapter, the gap settings of CAVs are controlled in a control region. However, CAVs that are not located in the control region remain uncontrolled and the gap setting is

chosen by the drivers. To reflect the heterogeneity of the drivers' preferences, this study reviewed related research (Nowakowski et al., 2010). The experiment, described in the research, offered ACC-equipped vehicles to the drivers for 13 days and asked the drivers to use the ACC mode while driving. The test results showed that the drivers chose the longest gap setting (2.2s) among the provided three gap settings (1.1s, 1.6s, and 2.2s) 20% of the time. Therefore, this study assumed that 20% of the drivers prefer long gap setting while the other 80% of the drivers prefer short gap setting.

4.1.3. Scenarios

To evaluate the effectiveness of the proposed strategy, this study compared the proposed strategy with uncontrolled case (no control) and merging control only. Also, to evaluate the effectiveness of the strategies on various demands, a simulation was conducted with three demand scenarios with a length of 90 minutes (**Figure 4.2**). The warm-up time was set as 5 minutes for all scenarios.

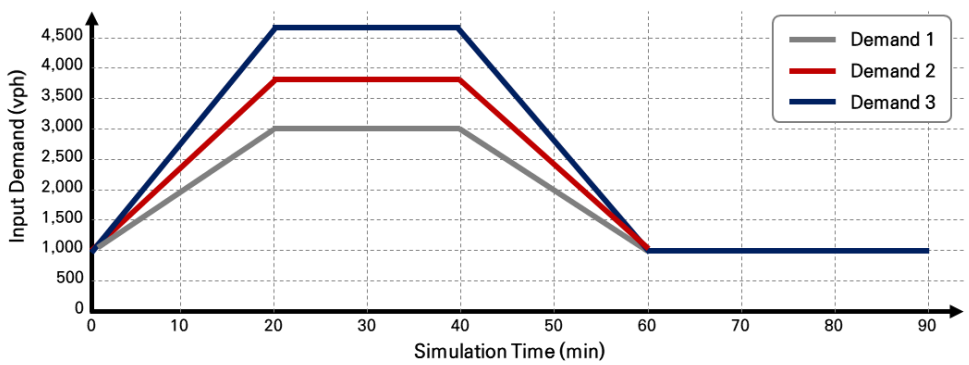

Figure 4.2. Demand scenarios

Also, it should be noted that CAVs and HDVs are expected to co-exist on the highway for a long time (Zhou et al., 2017; Karimi et al., 2020; Chen et al., 2021). Therefore, to evaluate the effectiveness of the proposed strategy in a mixed-flow, various market penetration rates (MPRs) of CAVs are evaluated: 1%, 3%, 10%, 20%, 30%, 40%, 50%, 60%, 70%, 80%, 90%, 97%, 99%, and 100%.

4.2. Results and Discussions

4.2.1. Results under CAV 100% Environment

To evaluate the operational benefits of the proposed strategies, average travel time of all vehicles traveled within the simulation network was calculated. Also, the standard deviation of speed was analyzed with the detector data located 100m upstream from the lane-dropping point. Note that each scenario was repeatedly simulated 30 times in order to consider the random effects of the simulation.

Table 4.5 summarizes the simulated results under three demand scenarios. Clearly, the results show that operating the proposed strategy can significantly improve the efficiency of the traffic flow in terms of travel time, regardless of the demand levels. The benefit increases with the increase in the demand level, and the results indicate that combining inflow control is necessary when the demand is high. Also, the standard deviation of speed is reduced by more than 50% for all demand scenarios when merging control is operated, indicating that the disruption due to mandatory lane changing is reduced significantly.

Table 4.5 Travel time and standard deviation of speed under CAV environment

Demand	Control	Avg. Travel Time (sec/veh)		Speed Std. Dev. (kph)	
		Value	% change	Value	% change
Demand 1	No control	190.2	-	17.8	-
	Merging control only	183.6	-3.5%	6.9	-61.0%
	Proposed strategy	183.6	-3.5%	6.9	-61.1%
Demand 2	No control	383.3	-	47.5	-
	Merging control only	186.7	-51.3%	7.4	-84.4%
	Proposed strategy	186.4	-51.4%	6.8	-85.7%
Demand 3	No control	736.7	-	39.5	-
	Merging control only	486.0	-34.0%	14.5	-63.2%
	Proposed strategy	284.8	-61.3%	7.9	-79.9%

The density heatmap for each scenario is shown in Figure 4.3.

For a high demand scenario (Demand 3), the queue forms from the lane-dropping point for no control whereas the starting point of the queue moves upstream, when the control is operated. Specifically, for merging control only, the queue forms from the starting point of section 2, and for the proposed strategy, the queue forms from the starting point of section 1. As a consequence, the density is kept low near the lane-dropping point. Both the maximum queue length and the duration of the congestion are reduced by operating the proposed strategy. Also, for Demand 2, operating merging control significantly lowers the density by enhancing merging with reduced disruption. For Demand 1, no difference can be found depending on whether the strategy was operated or not.

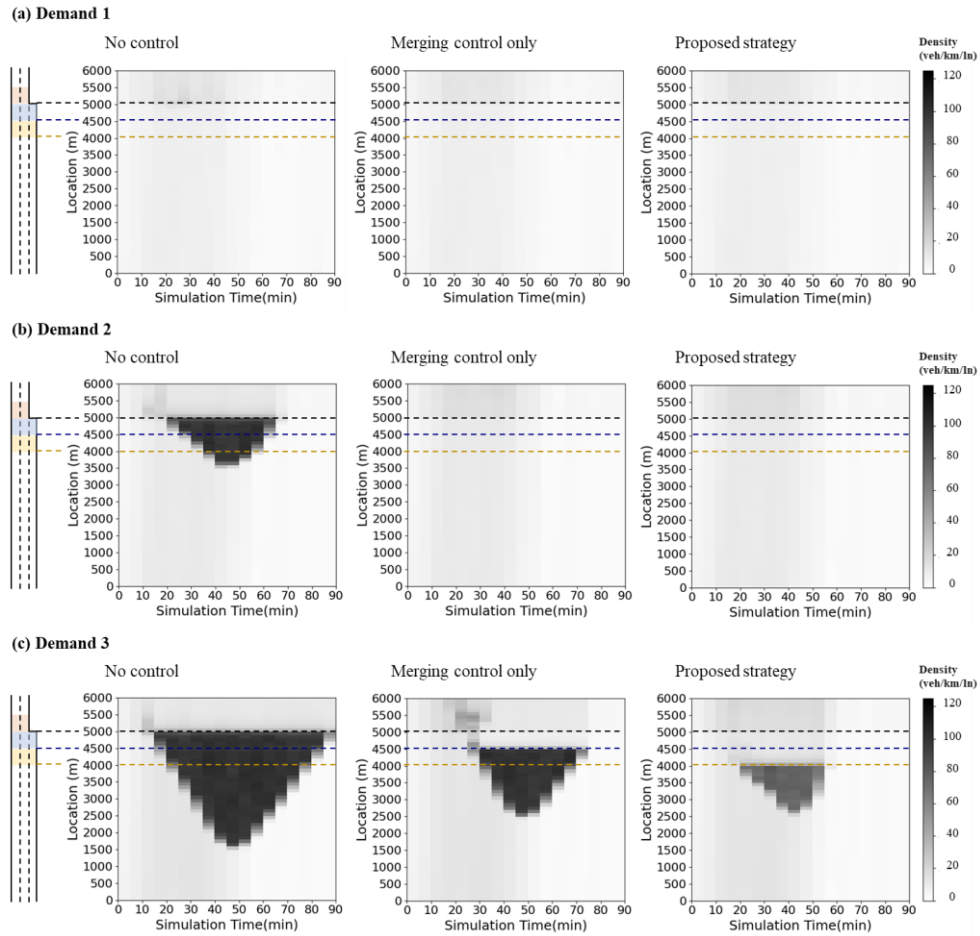

Figure 4.3. Density heatmap under CAV environment

However, it should be noted that keeping the density low does not guarantee an increase in throughput at the lane-drop bottleneck. The time-occupancy plot shown in Figure 4.4 demonstrates the result for the PID controller. The occupancy is collected every 10 seconds from the detector located upstream of the bottleneck. As explained in the previous section, inflow control uses a PID controller to keep the occupancy near the target occupancy and prevent the capacity drop. When merging control is operated without inflow control, it shows that the occupancy is not maintained at the target occupancy. This is because merging control is a rule-based microscopic control that does not guarantee optimized operation. For the proposed strategy, however, inflow control successfully controls the occupancy near target occupancy. As mentioned previously, target occupancy is set so that the throughput exceeds the original throughput without control. This guarantees the operational benefit when the proposed strategy is operated.

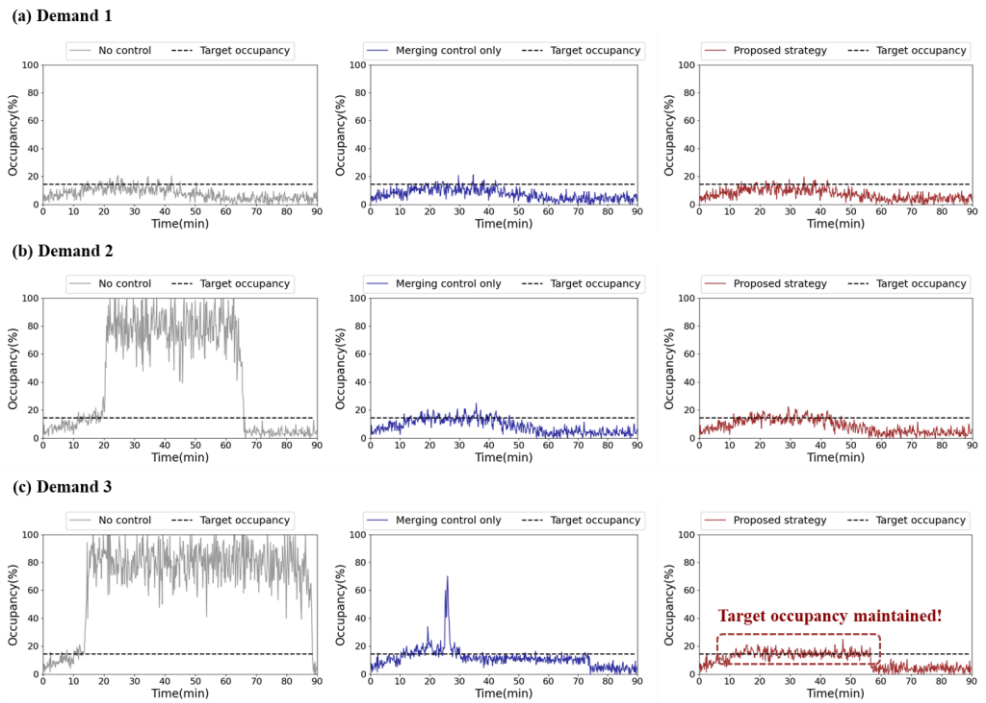

Figure 4.4. Occupancy-time plot under CAV environment

Figure 4.5 shows the throughput collected from the detector located 100m upstream from the lane-dropping point under demand 3. The throughput was aggregated every 60 seconds. The figure shows that capacity drop occurs in no control scenario. When merging control was operated without inflow control, capacity drop was delayed compared to no control, but the throughput was kept around 3,000vph before the queue dissipation. The proposed strategy successfully prevented the capacity drop and also kept throughput around 4,000vph, which is higher than the compared scenarios. The result verifies that when the occupancy is controlled properly by the PID controller, the throughput can be controlled high.

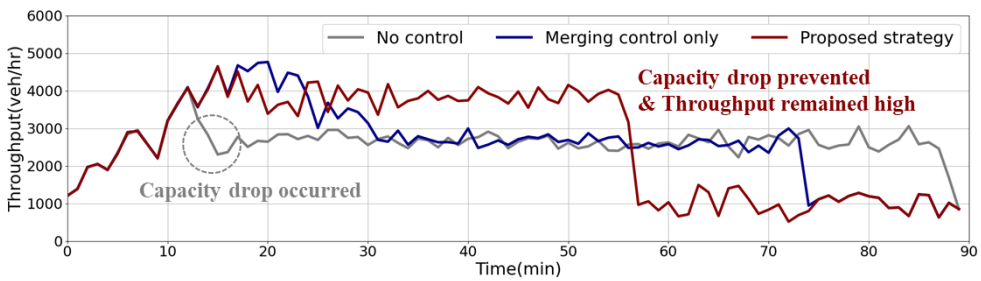

Figure 4.5. Throughput under CAV environment (Demand 3)

Other than the operational benefit of the traffic flow, the environmental benefit was also addressed (Table 4.6). Average CO_2 emissions was calculated by the Comprehensive Modal Emission Model (CMEM). The results show that the improvement in the environmental aspect was significant in high-demand scenarios (Demand 2, Demand 3), and the percent change was less than 1% in the lowest-demand scenario. The result implies that the environmental benefit increases with higher demands.

Table 4.6 CO_2 Emissions under CAV environment

Demand	Control	CO_2 Emissions (g/km)	
		Value	% change
Demand 1	No control	197.8	−
	Merging control only	197.7	−0.0%
	Proposed strategy	197.7	−0.0%
Demand 2	No control	215.2	−
	Merging control only	195.6	−9.1%
	Proposed strategy	195.6	−9.1%
Demand 3	No control	248.0	−
	Merging control only	224.2	−9.6%
	Proposed strategy	196.5	−20.8%

Also, Surrogate Safety Assessment Model 3 (SSAM3) was used to evaluate the safety improvement. In SSAM, the potential conflicts are considered if the Time−To−Collision (TTC) and the Post Encroachment Time (PET) values are lower than 1.5 seconds and 5.0 seconds, respectively (Rahman et al., 2019). The number of conflicts when the proposed strategy is operated was calculated and compared with that of no control and merging control only scenarios (Table 4.7). The results show that the number of conflicts reduces significantly when the proposed strategy is activated. Also, it should be noted that under low−demand scenarios (Demand 1 and Demand 2), both merging control only and the proposed strategy show their capability of nearly eliminating the conflicts caused by mandatory lane changing.

Table 4.7 Number of conflicts under CAV environment

Demand	Control	Number of Conflicts	
		Value	% change
Demand 1	No control	214	−
	Merging control only	0	−100.0%
	Proposed strategy	0	−100.0%
Demand 2	No control	2,632	−
	Merging control only	1	−100.0%
	Proposed strategy	0	−100.0%
Demand 3	No control	7,195	−
	Merging control only	3,886	−46.0%
	Proposed strategy	619	−91.4%

4.2.2. Results under Mixed Traffic Environment

CAVs and HDVs are expected to co-exist on the highway for a long time (Zhou et al., 2016; Karimi et al., 2020). Therefore, it is necessary to further investigate the performance of the proposed strategy in a mixed-traffic environment. For the evaluation under a mixed traffic environment, Demand 3 is selected since it is the most critical scenario. Various Market Penetration Rates (MPRs) were evaluated with 30 random seeds for each scenario.

As shown in **Figure 4.6** and **Table 4.8**, the travel time is reduced for all MPR scenarios when the control is operated. For the proposed strategy, the travel time reduction rate increases as the CAV MPR increases. This indicates that the traffic efficiency at the lane-drop bottleneck increases with more controllable CAVs. Furthermore, when CAV MPR is higher than 50%, the gain in performance is marginal. In other words, even with the coexistence of the unpredictable HDVs, the proposed strategy successfully improves efficiency with a minor loss in performance compared to a fully controllable environment. It is also interesting that the travel time reduction rate for MPRs lower than 50% does not show a difference between the merging control only and the proposed strategy. This implies that the inflow is not controlled sufficiently by controlling the gap settings of a limited number of vehicles upstream. When MPR is more than 50%, inflow control successfully further improves the traffic flow efficiency when operated with merging control.

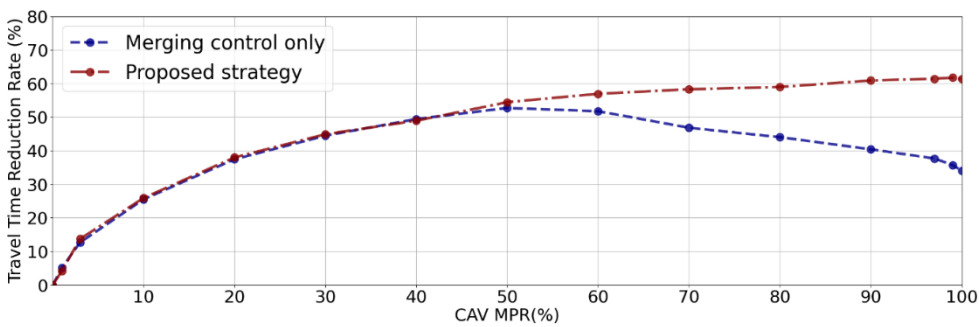

Figure 4.6. Travel time reduction rate with different MPRs

Table 4.8 Travel time and standard deviation of speed with different MPRs

MPR (%)	Control	Avg. Travel Time (sec/veh)		Speed Std. Dev. (kph)	
		Value	% change	Value	% change
1	No control	481.8	–	41.7	–
	Merging control only	457.3	−5.1%	40.9	−2.0%
	Proposed strategy	461.9	−4.1%	40.9	−2.0%
3	No control	496.1	–	41.9	–
	Merging control only	433.4	−12.6%	39.7	−5.1%
	Proposed strategy	428.1	−13.7%	39.7	−5.3%
10	No control	523.2	–	41.9	–
	Merging control only	389.7	−25.5%	37.8	−9.6%
	Proposed strategy	387.6	−25.9%	37.7	−9.9%
20	No control	558.1	–	41.7	–
	Merging control only	349.2	−37.4%	35.8	−14.3%
	Proposed strategy	346.0	−38.0%	35.7	−14.4%
30	No control	590.8	–	41.5	–
	Merging control only	328.1	−44.5%	34.2	−17.5%
	Proposed strategy	325.6	−44.9%	33.6	−18.9%
40	No control	615.6	–	41.3	–
	Merging control only	311.4	−49.4%	32.3	−21.6%
	Proposed strategy	314.4	−48.9%	31.9	−22.6%
50	No control	641.3	–	40.9	–
	Merging control only	303.3	−52.7%	27.1	−33.6%
	Proposed strategy	292.2	−54.4%	27.3	−33.2%
60	No control	666.6	–	40.5	–
	Merging control only	321.6	−51.7%	20.9	−48.4%
	Proposed strategy	287.0	−56.9%	15.7	−61.1%
70	No control	691.4	–	40.0	–
	Merging control only	367.7	−46.8%	19.0	−52.4%
	Proposed strategy	288.4	−58.3%	11.2	−72.1%
80	No control	713.5	–	39.7	–
	Merging control only	399.5	−44.0%	17.3	−56.3%
	Proposed strategy	292.7	−59.0%	7.3	−81.5%
90	No control	722.6	–	39.6	–
	Merging control only	430.7	−40.4%	16.9	−57.4%
	Proposed strategy	282.6	−60.9%	7.2	−81.8%
97	No control	732.5	–	39.6	–
	Merging control only	456.5	−37.7%	15.9	−59.9%
	Proposed strategy	282.5	−61.4%	7.9	−80.1%
99	No control	731.2	–	39.7	–
	Merging control only	470.2	−35.7%	14.8	−62.6%
	Proposed strategy	279.7	−61.7%	7.6	−80.9%
100	No control	736.7	–	39.5	–
	Merging control only	486.0	−34.0%	14.5	−63.2%
	Proposed strategy	284.8	−61.3%	7.9	−79.9%

The effectiveness of the proposed strategy under various MPR scenarios can be further discussed with a macroscopic fundamental diagram shown in Figure 4.7. As shown in Figure 4.7(a), for no control, the capacity drop occurs. Even when the input volume was high, the capacity drop is perfectly prevented with the operation of the proposed strategy. Also, when unpredictable HDVs coexist, the capacity drop can still be prevented for MPRs over 70%. Moreover, the red dots, indicating the operation of the proposed strategy, located in the congested regime is significantly reduced for MPRs higher than 50%. Figure 4.7(j) shows the effect of the proposed strategy for the MPR 10% scenario. Although the capacity drop is not prevented, the average density for the congested state is reduced significantly with higher throughput. This trend applies to the other MPR scenarios, which explains the reduction in travel time for all MPR scenarios as presented in Table 4.8.

The environmental and safety effects are also presented in Table 4.9 and Table 4.10, respectively. Both merging control only and the proposed strategy reduced CO_2 emissions, as well as the number of conflicts significantly for all MPRs. The results suggest that the proposed strategy is not only effective in improving traffic flow efficiency, but also has positive effects on environmental performance and safety.

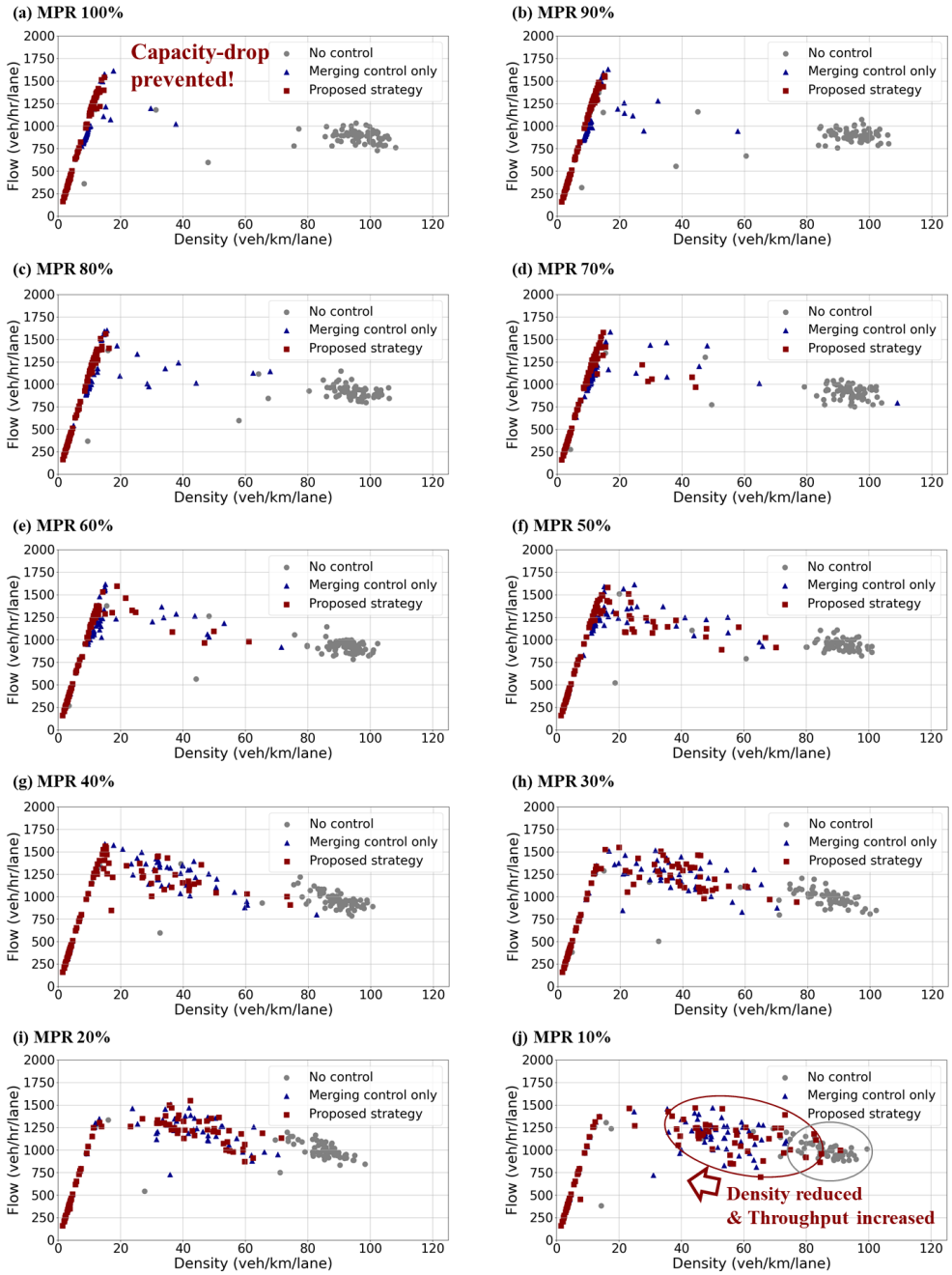

Figure 4.7. Flow–density curve with different MPRs

Table 4.9 CO_2 emissions with different MPRs

MPR (%)	Control	CO_2 Emissions (g/km) Value	% change
1	No control	223.4	–
	Merging control only	223.0	−0.2%
	Proposed strategy	222.2	−0.5%
3	No control	229.2	–
	Merging control only	221.1	−3.5%
	Proposed strategy	219.6	−4.2%
10	No control	233.3	–
	Merging control only	211.3	−9.4%
	Proposed strategy	211.2	−9.4%
20	No control	236.1	–
	Merging control only	206.2	−12.6%
	Proposed strategy	20.5	−12.9%
30	No control	241.2	–
	Merging control only	203.2	−15.8%
	Proposed strategy	200.8	−16.7%
40	No control	242.4	–
	Merging control only	200.8	−17.2%
	Proposed strategy	199.1	−17.9%
50	No control	247.6	–
	Merging control only	200.5	−19.0%
	Proposed strategy	197.8	−20.1%
60	No control	248.2	–
	Merging control only	204.3	−17.7%
	Proposed strategy	198.0	−20.2%
70	No control	250.8	–
	Merging control only	210.1	−16.2%
	Proposed strategy	198.2	−20.9%
80	No control	253.0	–
	Merging control only	215.2	−14.9%
	Proposed strategy	198.1	−21.7%
90	No control	248.4	–
	Merging control only	216.8	−12.7%
	Proposed strategy	196.5	−20.9%
97	No control	250.1	–
	Merging control only	221.4	−11.5%
	Proposed strategy	197.1	−21.2%
99	No control	249.8	–
	Merging control only	227.2	−9.1%
	Proposed strategy	197.7	−20.9%
100	No control	248.0	–
	Merging control only	224.2	−9.6%
	Proposed strategy	196.5	−20.8%

Table 4.10 Number of conflicts with different MPRs

MPR (%)	Control	Number of Conflicts Value	% change
1	No control	5,515	–
	Merging control only	5,086	−7.8%
	Proposed strategy	5,054	−8.4%
3	No control	5,955	–
	Merging control only	4,249	−28.7%
	Proposed strategy	4,170	−30.0%
10	No control	6,523	–
	Merging control only	3,237	−50.4%
	Proposed strategy	3,204	−50.9%
20	No control	6,539	–
	Merging control only	2,752	−57.9%
	Proposed strategy	2,634	−59.7%
30	No control	8,755	–
	Merging control only	2,744	−68.7%
	Proposed strategy	2,378	−72.8%
40	No control	9,662	–
	Merging control only	2,366	−75.5%
	Proposed strategy	2,132	−77.9%
50	No control	11,666	–
	Merging control only	2,771	−76.2%
	Proposed strategy	2,042	−82.5%
60	No control	12,414	–
	Merging control only	3,679	−70.4%
	Proposed strategy	1,572	−87.3%
70	No control	13,118	–
	Merging control only	5,191	−60.4%
	Proposed strategy	1,680	−87.2%
80	No control	13,085	–
	Merging control only	6,009	−54.1%
	Proposed strategy	1,445	−89.0%
90	No control	10,805	–
	Merging control only	5,465	−49.4%
	Proposed strategy	811	−92.5%
97	No control	9,336	–
	Merging control only	5,716	−38.8%
	Proposed strategy	737	−92.1%
99	No control	8,640	–
	Merging control only	5,412	−37.4%
	Proposed strategy	826	−90.4%
100	No control	7194	–
	Merging control only	3886	−46.0%
	Proposed strategy	619	−91.4%

Chapter 5. Conclusions

This study proposed a novel concept of controlling the gap setting of CAVs to improve throughput at a freeway lane-drop bottleneck. The proposed strategy consists of two parts: merging control and inflow control. Merging control is a microscopic control strategy that adjusts the gap setting of CAVs to a proposed gap setting to reduce disruption due to merging. The CAVs with a proposed gap setting not only follow the preceding vehicle in the same lane but also follow the preceding vehicle in the adjacent lane if the vehicle is present. Inflow control controls the gap settings of CAVs dynamically to regulate the upstream inflow and keep the bottleneck occupancy at the target occupancy. Proportional-Integral-Derivative (PID) controller was utilized for inflow control.

The effectiveness of the proposed strategy was evaluated using microsimulation VISSIM. The simulation results confirmed that the proposed strategy improved traffic flow efficiency near the lane-drop bottleneck under all demand scenarios in the CAV environment. Merging control of the proposed strategy could reduce the speed disturbance by more than 60% and inflow control could keep the occupancy at the target. Consequently, the proposed strategy successfully prevented capacity drop and improved flow efficiency. The proposed strategy also reduced CO_2 emissions and the number of conflicts under all demand scenarios.

The impact of the proposed strategy in a mixed-traffic environment was further analyzed. The results showed that the proposed strategy can improve the efficiency of the traffic flow for all MPRs, and the gain in performance was marginal for MPRs higher than 50%. The proposed strategy also reduced CO_2 emissions and the number of conflicts under all MPRs.

It should be noted that the only property controlled by the traffic management center for the proposed strategy is the gap settings of CAVs. This minimized control by the center allows being easily

implemented in the field in a technical aspect. Moreover, since the CAVs are only controlled in the control region, another strong advantage of the proposed strategy is its minimized need for infrastructure for the operation.

Bibliography

Aghabayk, K., Sarvi, M., & Young, W. (2015). A state-of-the-art review of car-following models with particular considerations of heavy vehicles. Transport reviews, 35(1), 82-105.

Bando, M., Hasebe, K., Nakayama, A., Shibata, A., & Sugiyama, Y. (1995). Dynamical model of traffic congestion and numerical simulation. Physical review E, 51(2), 1035.

Bang, S., & Ahn, S. (2018). Control of connected and autonomous vehicles with cut-in movement using spring mass damper system. Transportation Research Record, 2672(20), 133-143.

Cao, W., Mukai, M., Kawabe, T., Nishira, H., & Fujiki, N. (2015). Cooperative vehicle path generation during merging using model predictive control with real-time optimization. Control Engineering Practice, 34, 98-105.

Chen, N., van Arem, B., Alkim, T., & Wang, M. (2020). A hierarchical model-based optimization control approach for cooperative merging by connected automated vehicles. IEEE Transactions on Intelligent Transportation Systems, 22(12), 7712-7725.

Chen, T., Wang, M., Gong, S., Zhou, Y., & Ran, B. (2021). Connected and automated vehicle distributed control for on-ramp merging scenario: A virtual rotation approach. Transportation Research Part C: Emerging Technologies, 133, 103451.

Cho, H. W., & Laval, J. A. (2020). Combined ramp-metering and variable speed limit system for capacity drop control at merge bottlenecks. Journal of Transportation Engineering, Part A: Systems, 146(6), 04020033.

Davis, L. C. (2004). Effect of adaptive cruise control systems on traffic flow. Physical Review E, 69(6), 066110.

Guériau, M., Billot, R., El Faouzi, N. E., Monteil, J., Armetta, F., & Hassas, S. (2016). How to assess the benefits of connected vehicles? A simulation framework for the design of cooperative traffic management strategies. Transportation research part C: emerging technologies, 67, 266-279.

Gunter, G., Gloudemans, D., Stern, R. E., McQuade, S., Bhadani, R.,

Bunting, M., ... & Work, D. B. (2020). Are commercially implemented adaptive cruise control systems string stable?. IEEE Transactions on Intelligent Transportation Systems, 22(11), 6992-7003.

Guo, Y., Xu, H., Zhang, Y., & Yao, D. (2020). Integrated variable speed limits and lane-changing control for freeway lane-drop bottlenecks. IEEE Access, 8, 54710-54721.

Hu, Z., Huang, J., Yang, Z., & Zhong, Z. (2021). Embedding robust constraint-following control in cooperative on-ramp merging. IEEE Transactions on Vehicular Technology, 70(1), 133-145.

Hu, X., & Sun, J. (2019). Trajectory optimization of connected and autonomous vehicles at a multilane freeway merging area. Transportation Research Part C: Emerging Technologies, 101, 111-125.

Jiang, R., Wu, Q., & Zhu, Z. (2001). Full velocity difference model for a car-following theory. Physical Review E, 64(1), 017101.

Jin, H. Y., & Jin, W. L. (2015). Control of a lane-drop bottleneck through variable speed limits. Transportation Research Part C: Emerging Technologies, 58, 568-584.

Karimi, M., Roncoli, C., Alecsandru, C., & Papageorgiou, M. (2020). Cooperative merging control via trajectory optimization in mixed vehicular traffic. Transportation Research Part C: Emerging Technologies, 116, 102663.

Kesting, A., Treiber, M., & Helbing, D. (2010). Enhanced intelligent driver model to access the impact of driving strategies on traffic capacity. Philosophical Transactions of the Royal Society A: Mathematical, Physical and Engineering Sciences, 368(1928), 4585-4605.

Khondaker, B., & Kattan, L. (2015). Variable speed limit: A microscopic analysis in a connected vehicle environment. Transportation Research Part C: Emerging Technologies, 58, 146-159.

Liang, J., Guan, T., Liu, D., Liu, X., Luan, Z., Liu, H., & Yuan, X. (2022). An optimal trajectory planning for automated on-ramp

merging. IET Intelligent Transport Systems.

Lu, X. Y., & Hedrick, J. K. (2003). Longitudinal control algorithm for automated vehicle merging. International Journal of Control, 76(2), 193-202.

Makridis, M., Mattas, K., Ciuffo, B., Re, F., Kriston, A., Minarini, F., & Rognelund, G. (2020). Empirical study on the properties of adaptive cruise control systems and their impact on traffic flow and string stability. Transportation research record, 2674(4), 471-484.

Milanés, V., & Shladover, S. E. (2014). Modeling cooperative and autonomous adaptive cruise control dynamic responses using experimental data. Transportation Research Part C: Emerging Technologies, 48, 285-300.

Min, H., Fang, Y., Wang, R., Li, X., Xu, Z., & Zhao, X. (2020). A novel on-ramp merging strategy for connected and automated vehicles based on game theory. Journal of Advanced Transportation, 2020.

Monteil, J., Bouroche, M., & Leith, D. J. (2018). $\mathcal{L}_2$ and $\mathcal{L}_\infty$ Stability Analysis of Heterogeneous Traffic With Application to Parameter Optimization for the Control of Automated Vehicles. IEEE Transactions on Control Systems Technology, 27(3), 934-949.

Müller, E. R., Carlson, R. C., Kraus, W., & Papageorgiou, M. (2015). Microsimulation analysis of practical aspects of traffic control with variable speed limits. IEEE Transactions on Intelligent Transportation Systems, 16(1), 512-523.

Nowakowski, C., O'Connell, J., Shladover, S. E., & Cody, D. (2010, September). Cooperative adaptive cruise control: Driver acceptance of following gap settings less than one second. In Proceedings of the Human Factors and Ergonomics Society Annual Meeting (54, 24, 2033-2037)

Papageorgiou, M., Hadj-Salem, H., & Blosseville, J. M. (1991). ALINEA: A local feedback control law for on-ramp metering. Transportation research record, 1320(1), 58-67.

Punzo, V., Zheng, Z., & Montanino, M. (2021). About calibration of car-following dynamics of automated and human-driven vehicles: Methodology, guidelines and codes. Transportation

Research Part C: Emerging Technologies, 128, 103165.
Rahman, M. S., Abdel-Aty, M., Lee, J., & Rahman, M. H. (2019). Safety benefits of arterials' crash risk under connected and automated vehicles. Transportation Research Part C: Emerging Technologies, 100, 354-371.
Ren, T., Xie, Y., & Jiang, L. (2020). Cooperative highway work zone merge control based on reinforcement learning in a connected and automated environment. Transportation research record, 2674(10), 363-374.
Ren, T., Xie, Y., & Jiang, L. (2021). New England merge: a novel cooperative merge control method for improving highway work zone mobility and safety. Journal of Intelligent Transportation Systems, 25(1), 107-121.
Rios-Torres, J., & Malikopoulos, A. A. (2016). A survey on the coordination of connected and automated vehicles at intersections and merging at highway on-ramps. IEEE Transactions on Intelligent Transportation Systems, 18(5), 1066-1077.
Shang, M., & Stern, R. E. (2021). Impacts of commercially available adaptive cruise control vehicles on highway stability and throughput. Transportation research part C: emerging technologies, 122, 102897.
Shi, X., & Li, X. (2021). Empirical study on car-following characteristics of commercial automated vehicles with different headway settings. Transportation research part C: emerging technologies, 128, 103134.
Sun, J., Zheng, Z., & Sun, J. (2018). Stability analysis methods and their applicability to car-following models in conventional and connected environments. Transportation research part B: methodological, 109, 212-237.
Talebpour, A., & Mahmassani, H. S. (2016). Influence of connected and autonomous vehicles on traffic flow stability and throughput. Transportation Research Part C: Emerging Technologies, 71, 143-163.
Treiber, M., & Kesting, A. (2013). Traffic flow dynamics. Traffic

Flow Dynamics: Data, Models and Simulation, Springer-Verlag Berlin Heidelberg, 983-1000.

Wang, Y., Kosmatopoulos, E. B., Papageorgiou, M., & Papamichail, I. (2014). Local ramp metering in the presence of a distant downstream bottleneck: Theoretical analysis and simulation study. IEEE Transactions on Intelligent Transportation Systems, 15(5), 2024-2039.

Wang, Z., Wu, G., & Barth, M. (2018). Distributed consensus-based cooperative highway on-ramp merging using V2X communications (No. 2018-01-1177). SAE Technical Paper.

Wu, Y., Tan, H., Qin, L., & Ran, B. (2020). Differential variable speed limits control for freeway recurrent bottlenecks via deep actor-critic algorithm. Transportation research part C: emerging technologies, 117, 102649.

Yao, Z., Xu, T., Jiang, Y., & Hu, R. (2021). Linear stability analysis of heterogeneous traffic flow considering degradations of connected automated vehicles and reaction time. Physica A: Statistical Mechanics and Its Applications, 561, 125218.

Yuan, K., Knoop, V. L., & Hoogendoorn, S. P. (2015). Capacity drop: Relationship between speed in congestion and the queue discharge rate. Transportation Research Record, 2491(1), 72-80.

Zhang, Y., & Ioannou, P. A. (2016). Combined variable speed limit and lane change control for highway traffic. IEEE Transactions on Intelligent Transportation Systems, 18(7), 1812-1823.

Zheng, Y., Wang, J., & Li, K. (2020). Smoothing traffic flow via control of autonomous vehicles. IEEE Internet of Things Journal, 7(5), 3882-3896.

Zhou, M., Qu, X., & Jin, S. (2016). On the impact of cooperative autonomous vehicles in improving freeway merging: a modified intelligent driver model-based approach. IEEE Transactions on Intelligent Transportation Systems, 18(6), 1422-1428.

Zhou, Y., Cholette, M. E., Bhaskar, A., & Chung, E. (2018). Optimal vehicle trajectory planning with control constraints and recursive implementation for automated on-ramp merging. IEEE

Transactions on Intelligent Transportation Systems, 20(9), 3409-3420.

Zhu, J., Easa, S., & Gao, K. (2022). Merging control strategies of connected and autonomous vehicles at freeway on-ramps: a comprehensive review. Journal of Intelligent and Connected Vehicles.

Zhu, W. X., & Zhang, H. M. (2018). Analysis of mixed traffic flow with human-driving and autonomous cars based on car-following model. Physica A: Statistical Mechanics and its Applications, 496, 274-285.

Abstract

차로감소 병목구간은 차로감소, 공사, 사고 등으로 인해 고속도로에서 자주 관측된다. 이러한 고속도로 차로감소 병목구간에서는 필수적인 차로변경으로 인한 차들 간의 상충, 그리고 상류부 유입교통량이 하류부 용량보다 큰 상황으로 인해 용량저하가 발생할 수 있다. 따라서 CAV 제어를 통해 차량 합류 행태를 개선하고 상류부 유입교통량을 조절할 수 있다면 정체구간 유출교통량을 늘릴 수 있을 것으로 기대된다. 본 연구는 CAV가 현재 판매되는 자율주행차들이 제공하는 차간거리설정을 포함하여 여러 차간거리설정들을 제공한다고 가정하였으며, CAV의 차간거리설정 제어를 통해 차로감소 병목구간의 유출교통량을 증가시킬 수 있는 새로운 개념의 전략을 제안하였다. 본 연구에서 제안하는 전략은 합류제어와 유입량제어로 구성된다. 합류제어는 CAV의 차간거리설정을 합류를 개선할 수 있도록 제안된 새로운 차간거리설정으로 조정한다. 유입량제어는 비례-적분-미분 제어기를 활용하여 CAV들의 차간거리설정을 가장 긴 설정 혹은 가장 짧은 설정으로 동적으로 제어함으로써 상류부 유입교통량을 조절하고 병목구간 점유율을 목표 점유율에 가깝게 유지하도록 한다. 본 연구는 제안된 전략의 성능을 평가하기 위해 미시교통류시뮬레이션 VISSIM에 전략을 구현하고 시뮬레이션을 진행하였다. 시뮬레이션 결과, CAV 환경에서 본 전략은 모든 용량 시나리오에 대해 용량저하를 방지하고 운영성을 개선하였다. 또한 본 전략은 검토된 모든 CAV 시장점유율에서 운영성을 개선하였고, 시장점유율 50% 이상에서는 개선 정도의 증가율이 미미함을 확인하였다. 운영성 뿐만 아니라 환경성과 안전성 측면에서도 모든 시장점유율에서 전략이 효과적임을 확인하였다.

주요어: 차간거리설정, 자율협력주행자동차, 차로감소 병목구간, 비례-적분-미분 제어, VISSIM
학 번: 2019-27105